Causes of atmospheric temperature change 1960-2000: A combined attribution analysis

Causes of atmospheric temperature change 1960–2000: A combined attribution analysis

Gareth S. Jones, Simon F. B. Tett, and Peter A. Stott

Met Office, Hadley Centre for Climate Prediction and Research, Bracknell, UK

Received 2 October 2002; revised 27 November 2002; accepted 24 December 2002; published 11 March 2003.

[1] We investigate the causes of temperature change over the last four decades, both near the surface and in the free atmosphere, using a coupled atmosphere/ocean general circulation model, HadCM3, which requires no flux correction. We use an 'optimal detection' methodology to examine zonal mean temperatures near the surface and on nine diagnosed pressure levels throughout the atmosphere over the last four decades of the 20th Century. This produces a space-time-multivariable detection analysis which for the first time includes both solar and volcanic forcings in addition to anthropogenic forcings. Our results strengthen the case for an anthropogenic influence on climate. Unlike previous studies we attribute observed decadal-mean temperature changes both to anthropogenic emissions, and changes in stratospheric volcanic aerosols. The temperature response to change in solar irradiance is also detected but with a lower confidence than the other forcings. *INDEX TERMS:* 1610 Global Change: Atmosphere (0315, 0325); 1620 Global Change: Climate dynamics (3309); 1650 Global Change: Solar variability; 3309 Meteorology and Atmospheric Dynamics: Climatology (1620); 8409 Volcanology: Atmospheric effects (0370). **Citation:** Jones, G. S., S. F. B. Tett, and P. A. Stott, Causes of atmospheric temperature change 1960–2000: A combined attribution analysis, *Geophys. Res. Lett.*, *30*(5), 1228, doi:10.1029/2002GL016377, 2003.

1. Introduction

[2] Recent detection and attribution studies [*Santer et al.*, 1996; *Hegerl et al.*, 1997; *Tett et al.*, 1999; *Gillett et al.*, 2000; *North and Wu*, 2001; *Stott et al.*, 2001; *Hill et al.*, 2001; *Tett et al.*, 2002] detected significant temperature changes in the free atmosphere and near the surface during the 20th century and attributed these changes largely to anthropogenic effects. A number of these studies used forms of 'optimal fingerprinting' [*Hasselmann*, 1997; *North and Stevens*, 1998; *Allen and Tett*, 1999], a method which optimises pattern variability, and we use a variant of this technique here.

[3] The 20th century near surface temperature record has been analysed by a variety of authors who have considered either trends of spatial patterns [e.g., *Hegerl et al.*, 1997] or spatio-temporal patterns on either decadal timescales [*Tett et al.*, 1999; *Stott et al.*, 2001; *Tett et al.*, 2002] or annual timescales [*Stott et al.*, 2001; *North and Wu*, 2001]. Their results varied depending on details of the analysis: the influence of anthropogenic climate forcings has dominated on decadal timescales, incorporation of seasonal information has made it easier to detect the weaker solar signals in the early part of the century and volcanic signals have been detected on annual timescales [*Stott et al.*, 2001; *North and Wu*, 2001]. In the free atmosphere trends of spatial patterns, over the last 40 years of the 20th century, rather than spatio-temporal patterns, have so far been analysed [*Santer et al.*, 1996; *Tett et al.*, 1996; *Allen and Tett*, 1999; *Hill et al.*, 2001].

[4] Here we extend these analyses by regressing simulated atmospheric temperature changes against the observational atmospheric temperature changes using decadal means of zonally averaged temperatures on nine diagnosed pressure levels from 1960 to 2000 in combination with changes in near surface temperatures.

2. Data

[5] We ran several ensembles of HadCM3, a non flux-adjusted ocean-atmosphere general circulation model, [*Gordon et al.*, 2000; *Pope et al.*, 2000] driven by different forcings, which include the most important anthropogenic forcings and the most important natural forcings [*Mitchell et al.*, 2001]. These we compare with the observed near-surface temperature changes (updated surface temperature dataset [*Parker et al.*, 1994]) and HadRT2.1s radiosonde temperature dataset [*Parker et al.*, 1997].

[6] We compute full monthly mean spatial field temperature anomalies on nine pressure levels (850, 700, 500, 300, 200, 150, 100, 50, 30 hPa) and near the surface (1.5 m) with respect to the 1960–1999 mean. The temperatures on pressure levels and near the surface are regridded and interpolated to the observational $5^\circ \times 5^\circ$ grid. Simulated data are discarded where there are no observational data. We process all the data identically and analyse the 40 year period 1960–1999. We compile observed annual means from an average of the monthly mean data with at least 4 months worth of data per year at any point.

[7] As we are trying to resolve a finer temporal structure than previous studies of the free atmosphere, the limited radiosonde coverage precludes a finer spatial structure. We average over three equal area latitudinal zones on each pressure level: 90°N–30°N, 30°N–0° and 0°–30°S. The 30°S–90°S zone is disregarded as there are very little observational data in this zone. From the annual data we compute ten year averages for the period 1960–1999. Any amount of missing data is allowed, although the periods and zones are such that there is always at least one observation in each zone, in each decade and on each level. Each level is mass weighted, calculated as the pressure difference between that level and the level below [*Tett et al.*, 1996]. The near surface data are weighted with the same weighting as the first free atmosphere level: 850 hPa.

Table 1. Naming Convention and Descriptions of the HadCM3 Ensembles

GHG	Response to well-mixed greenhouse gases including CO_2 and CH_4.
ANTHRO	As GHG with tropospheric and stratospheric ozone, and sulphur emissions. The indirect effect of sulphate aerosol was also taken into account.
NATURAL	Response to volcanic and solar forcings.
SOL	Response to solar irradiance [*Lean et al.*, 1995].
VOL	Response to volcanically produced stratospheric aerosols [*Sato et al.*, 1993].
ALL	Response to anthropogenic and natural forcings.
CONTROL	Control simulation, 1120 years (at time of this analysis) with constant external forcing.

Apart from CONTROL, each ensemble comprised of four members, each initialised with different start conditions.

[8] The HadCM3 simulations we use in this analysis are described in Table 1 (More information on these simulations can be found in *Stott et al.* [2000] and *Tett et al.* [2002].)

3. Optimal Detection Methodology

[9] 'Optimal' detection is multiple regression between a set of signals (derived in our case from model simulations) and observations, with optimisation [*Allen and Tett*, 1999]. The observations (y_i) are assumed to be a linear combination of scaled climate forcing signals (x_i) and internal climate variability

$$y = \sum_i \beta_i x_i + u \quad (1)$$

[10] The analysis is optimised by projecting the observations, signals and noise onto the leading eigenvectors of an estimate of the noise covariance matrix (in our case calculated from the CONTROL) and by weighting down those spatio-temporal patterns of temperature change with high variability and weighting up those with low variability. Different permutations of the projected signal patterns are then regressed against the projected observations creating sets of regression coefficients (amplitudes). Further details of optimal detection are described elsewhere [*Tett et al.*, 1999; *Stott et al.*, 2001; *Tett et al.*, 2002]. (Apart from the preprocessing of the data as described above the precise methodology is as described in *Tett et al.* [2002]).

[11] We calculate the number of degrees of freedom of the optimised eigenvector space, estimated from the number of independent 40 year segments in CONTROL [times 1.5 *Tett et al.*, 2002] to be 42. We test the hypothesis that the residuals of the regression are consistent with our estimate of internal variability using an F-test [*Allen and Tett*, 1999]. We estimate the noise using intra-ensemble variability (i.e., the variability of the simulations about the ensemble mean) of the forced ensembles [*Tett et al.*, 2002] GHG, ANTHRO, NATURAL and ALL. The distribution of the residuals will depend on the amplitude of the forced signals [*Tett et al.*, 2002].

[12] We use the value of the F-test to determine (if possible) the choice of the total number of eigenvectors to be used in the optimisation (the truncation) by rejecting those truncations of the space where the F-test probability is outside the of 5–95% range.

[13] The simulations using anthropogenic forcings can be linearly combined to find *G* (response to well-mixed greenhouse gases) and *SO* (combined response to changes in sulphate aerosol and tropospheric and stratospheric ozone) [*Tett et al.*, 2002]. Standard tests are applied to the signal combinations to deduce how many of these signals are degenerate to each other [*Mardia et al.*, 1979, pp. 243–248].

4. Results

[14] We analyse contributions of *G*, *SO*, SOL and VOL to observed temperature change. Tests show that the signals are not degenerate. The amplitudes are given in Table 2 for *G*, *SO*, SOL and VOL for a truncated space of 20 eigenvectors (a truncation of 20). All four signals are detected and have amplitudes that are consistent with one. The truncated observations capture 92 percent of the variability of the untruncated observations. The detections of *G*, *SO* and VOL are robust over the range of allowed truncations (not shown here), but SOL is only detected for less than half of the available truncations.

[15] We reconstruct the temperature patterns on each of the atmospheric levels and at the surface with the relevant measured signal amplitudes for *G*, *SO*, SOL and VOL. Figure 1 shows the global mean reconstructed decadally averaged temperatures for the near surface, troposphere and stratosphere. The best fit is the sum of the simulated reconstructed temperatures. (We calculate the observational uncertainty range using the intra-ensemble variability described earlier.) The best fit matches the observed temperature changes quite accurately on all the levels. The filtered observations warm by 0.39 ± 0.16°C near the surface and 0.39 ± 0.15°C in the tropospheric temperatures, whilst the stratospheric temperatures cool by 1.30 ± 0.08°C, over the 40 years.

[16] *G* is the dominant contributor to the 40 year near surface and tropospheric temperature trends contributing 0.56 ± 0.15°C and 0.74 ± 0.20°C warming respectively (the uncertainties in the temperature trends are calculated from the signal amplitude uncertainties). *SO* contributes cooling trends of 0.10 ± 0.01°C and 0.18 ± 0.02°C to near surface and tropospheric temperatures respectively. VOL contributes a cooling of 0.09 ± 0.04°C and 0.14 ± 0.07°C to the near surface and tropospheric temperatures respectively, almost all in the last decade due to the 1991 Mount Pinatubo eruption. In this reconstruction SOL warms by

Table 2. Amplitudes and Signal to Noise Ratios

Climate signal	Regressed against Observation	Regressed against ALL ensemble	SNR
a) *G*	0.81[a] ± 0.24 (0.27)	0.94[a] ± 0.12 (0.16)	4.63
SO	1.07[a] ± 0.10 (0.11)	0.87[a] ± 0.05 (0.07)	4.00
SOL	1.33[a] ± 0.77 (0.86)	0.13 ± 0.38 (0.54)	1.48
VOL	1.12[a] ± 0.39 (0.43)	0.64[a] ± 0.19 (0.27)	2.16
b) ALL	1.24[a] ± 0.13(0.14)		6.56

[a]Detection of signal.

a) (SNR) of *G*, *SO*, SOL and VOL Signals in Regression Against the Observations and Against ALL Ensemble Average as Surrogate Observations, Truncation of 20. b) Amplitude of the ALL Signal Against the Observations. Truncation of 15. Uncertainty Ranges Given as 90% Limits. Values in Brackets are Uncertainties Calculated for Null Hypothesis of Signal Amplitudes Equal to 1.

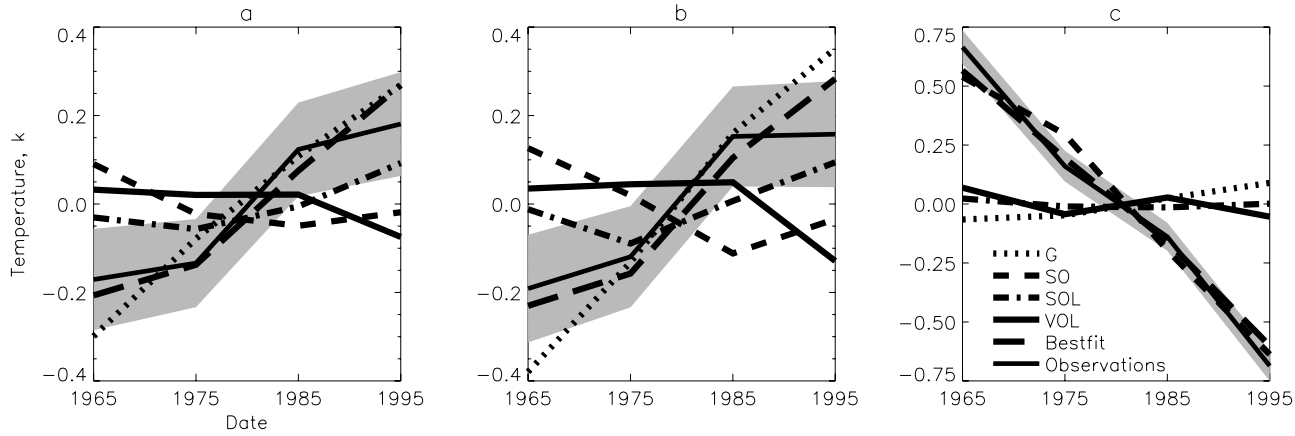

Figure 1. Global mean reconstructions of the scaled (Table 2) *G*, *SO*, SOL and VOL signals when regressed against the filtered observations. Temperatures expressed relative to 1960–1999. a) near surface temperatures. b) Tropospheric temperatures, average over zones and levels below the tropopause. c) Stratospheric temperatures, average over zones and levels above the tropopause. The best fit is the sum of the simulated reconstructed temperatures. The shaded area represents the uncertainty range on the observed temperatures, at the two standard deviation level.

0.12 ± 0.11°C in both the near surface and the troposphere over the 40 years. For the stratosphere *SO* is by far the most dominant, cooling by 1.20 ± 0.11°C. As *S* has no influence on the stratosphere the stratospheric ozone component of *SO* causes this temperature change [*Tett et al.*, 2002]. The other forcings have much smaller contributions in comparison (The warming from G in the stratosphere is due predominantly to a warming region in the model over the North polar region [*Tett et al.*, 2002]).

[17] At this truncation some important modes of variability are not being captured. This can be seen in the near surface temperature reconstruction (Figure 1). The observational temperature changes near the surface appear to go through a period of warming in the 1980's with less warming during the 1990's. In the untruncated observations (not shown here), the observations during the 1990's warm by as much as the warming in the 1980's. The fact that some changes in space and time are not being captured particularly well should be born in mind when examining Figure 1.

[18] We examine whether there are any important biases in the analysis by using the ensemble average of ALL as a surrogate for the observations, thus having a perfect model study. The covariance matrix used to calculate the uncertainty of the amplitudes, in this case estimated from inter-ensemble variability, is scaled by 1/4 to take into account the four member surrogate observation. Amplitudes are shown in Table 2. *G*, *SO*, and VOL are detected with only *G* having an amplitude that is consistent with an amplitude of unity. This demonstrates that there is some bias [*Mardia et al.*, 1979; *Allen and Tett*, 1999; *Stott et al.*, 2003a] as we would expect a priori to have all the amplitudes to be consistent with 1. The detections of *G* and *SO* are robust to the choice of truncation (not shown here), VOL is not quite as robustly detected, and SOL is not detected at all. There appears to be quite a difference between these amplitudes and those calculated from the regression against the observations. In particular SOL has a much higher amplitude in the observations than in ALL.

[19] We applied a test to find if the amplitudes from the regressions against the observations and against ALL were consistent with each other, by combining the covariance matrices from the two regressions. We found that the sets of amplitudes were not consistent with each other. Examining the individual signal amplitudes, and thus not involving how they covary with the other signals, we found that they were all also not consistent with their counterparts, apart from *G*. However there is a small range of low truncations which do give amplitudes from the two regressions which are consistent with each other.

[20] We measured the signal to noise ratio (SNR) for each signal (method described in *Tett et al.* [2002]), the values of which are given in Table 2. *G* and *SO* have large SNRs, 4.63 and 4.00 respectively, VOL has a SNR of 2.16 whilst SOL has the lowest SNR of 1.48. Using a statistical test [*Tett et al.*, 2002] we calculate that all four signals have signal to noise significantly greater than one at the 90% level, where a SNR of 1 would imply that just noise was present. The detection scheme could underestimate the amplitudes of signals with low SNR [*Mardia et al.*, 1979; *Allen and Tett*, 1999; *Stott et al.*, 2003a] which could explain the low amplitude of SOL when regressed against ALL even though we know that the same solar forcing exists in ALL as in SOL. Nevertheless we find that SOL is detected in the observations (albeit not robustly with truncation) with an amplitude whose best estimate is greater than, although still consistent with, 1. In the context that SOL is not detected in ALL and the known bias in amplitudes of signals with low SNR, this could be explained by there being a larger solar component in the observations than in the all forcings simulation [*Stott et al.*, 2003b]. The same could be said, to a lesser extent, for *SO* and VOL.

[21] We analyse contributions of ALL to observed change. Assuming linearity, this sets the relative amplitudes of the individual components of ALL (the anthropogenic and natural forcings) to be constant relative to each other, i.e., effectively the relative amplitudes are decided upon a priori. The ALL signal is detected across a small range of truncations up to a truncation of 15, the amplitude and

uncertainties are shown in Table 2. The amplitude is consistent with unity for the whole range of allowed truncations bar the maximum allowed truncation of 15. At this truncation the amplitude of ALL has an amplitude of 1.24 and is larger and not consistent with an amplitude of unity. This suggests that at the maximum truncation ALL underestimates the observed record. The truncated observations capture 90 percent of the variability of the untruncated observations at the maximum allowed truncation and the signal has a high measured SNR of 6.56.

5. Conclusions and Comments

[22] We have applied a spatio-temporal optimal detection scheme to decadal changes in the temperatures near the surface and in the free atmosphere on 9 different levels over the last 40 years of the 20th century. Simulations from a coupled ocean-atmosphere general circulation model, HadCM3, forced with different external climate forcing factors, were used to examine the major contributions to changes in atmospheric temperatures between 1960 and 1999.

[23] Both anthropogenic signals, *G* and *SO*, are robustly detected. Natural forcings are also detected, but solar irradiance changes are not as robustly detected as volcanic stratospheric aerosol changes. The range of amplitudes of SOL is large allowing amplitudes as low as 0.5 and as high as 2. Only one timeseries of solar irradiance changes was used in this analysis [*Lean et al.*, 1995] and other equally plausible reconstructions of solar irradiance changes throughout the twentieth century [e.g., *Hoyt and Schatten*, 1993] exist. The combination of signals that has the most explanatory power includes well-mixed greenhouse gases, other anthropogenic forcings, solar irradiance changes and volcanic stratospheric aerosol changes.

[24] Detection of anthropogenic signals in the work described here supports the findings of previous work using near surface temperatures [*Tett et al.*, 1999; *Stott et al.*, 2001; *Tett et al.*, 2002] and using free atmosphere temperatures [*Santer et al.*, 1996; *Tett et al.*, 1996; *Hill et al.*, 2001]. Unlike those studies, this detection of anthropogenic signals is found when both solar and volcanic signals are included. For the first time volcanic signals have been detected in the late 20th century temperature record on decadal timescales.

[25] Combining the near surface temperature with the free atmosphere temperature records has enabled the detection of weak signals that otherwise would not be detected near the surface or in the free atmosphere alone. This analysis demonstrates the advantage of combining different climate variable datasets over analysing those variables in isolation.

[26] **Acknowledgments.** Financial support to carry out the simulations and fund the authors was provided by U.K. Dept. for Environment, Food and Rural Affairs contract PECD 7/12/37. Supplementary support was provided by European Comission contract ENV4-CT97-0501 (QUARCC). We would also like to thank Tim Johns for running the CONTROL and several of the ANTHRO simulations and the reviewers of this paper for their useful comments.

References

Allen, M. R., and S. F. B. Tett, Checking for model consistency in optimal fingerprinting, *Clim. Dyn.*, *15*, 419–434, 1999.

Gillett, N. P., G. Hegerl, M. R. Allen, and P. Stott, Implications of changes in the Northern Hemisphere circulation for the detection of anthropogenic climate, *Geophys. Res. Lett.*, *27*, 993–996, 2000.

Gordon, C., et al., The simulation of SST, sea ice extents and ocean heat transports in a version of the Hadley Centre coupled model without flux adjustments, *Clim. Dyn.*, *16*, 147–168, 2000.

Hasselmann, K., Multi-pattern fingerprint method for detection and attribution of climate change, *Clim. Dyn.*, *13*, 601–612, 1997.

Hegerl, G. C., et al., Multi-fingerprint detection and attribution analysis of greenhouse gas, greenhouse gas-plus-aerosol and solar forced climate change, *Clim. Dyn.*, *13*, 613–634, 1997.

Hill, D. C., M. R. Allen, and P. A. Stott, Allowing for solar forcing in the detection of human influence on atmospheric vertical structure, *Geophys. Res. Lett.*, *28*, 1555–1558, 2001.

Hoyt, D. V., and K. H. Schatten, A discussion of plausible solar irradiance variations, 1700–1992, *J. Geophys. Res.*, *98*, 18,895–18,906, 1993.

Lean, J., J. Beer, and R. Bradley, Reconstruction of solar irradiance since 1610: Implications for climate change, *Geophys. Res. Lett.*, *22*, 3195–3198, 1995.

Mardia, K. V., J. T. Kent, and J. M. Bibby, *Multivariate Analysis*, Academic, San Diego, Calif., 1979.

Mitchell, J., D. Karoly, G. Hegerl, F. Zwiers, M. Allen, and J. Marengo, Detection of climate change and attribution of causes, in *Climate Change 2001: The Scientific Basis: Contribution of Working Group I to the Third Assessment Report of the Intergovernmental Panel on Climate Change*, edited by J. T. Houghton et al., pp. 695–738, Cambridge Univ. Press, New York, 2001.

North, G. R., and M. J. Stevens, Detecting climate signals in the surface temperature record, *J. Clim.*, *11*, 563–577, 1998.

North, G. R., and Q. Wu, Detecting climate signals using space-time eofs, *J. Clim.*, *14*, 1839–1863, 2001.

Parker, D. E., P. D. Jones, C. K. Folland, and A. Bevan, Interdecadal changes of surface temperature since the late nineteenth century, *J. Geophys. Res.*, *99*, 14,373–14,399, 1994.

Parker, D. E., et al., A new global gridded radiosonde temperature data base and recent temperature trends, *Geophys. Res. Lett.*, *24*, 1499–1502, 1997.

Pope, V. D., M. L. Gallani, P. R. Rowntree, and R. A. Stratton, The impact of new physical parametrizations in the Hadley Centre climate model-hadam3, *Clim. Dyn.*, *16*, 123–146, 2000.

Santer, B. D., et al., A search for human influences on the thermal structure of the atmosphere, *Nature*, *382*, 39–45, 1996.

Sato, M., J. E. Hansen, M. P. McCormick, and J. B. Pollack, Stratospheric aerosol optical depths (1850–1990), *J. Geophys. Res.*, *98*, 22,987–22,994, 1993.

Stott, P. A., S. F. B. Tett, G. S. Jones, M. R. Allen, J. F. B. Mitchell, and G. J. Jenkins, External control of 20th century temperature by natural and anthropogenic forcing, *Science*, *290*, 2133–2137, 2000.

Stott, P. A., S. F. B. Tett, G. S. Jones, M. R. Allen, W. J. Ingram, and J. F. B. Mitchell, Attribution of twentieth century temperature change to natural and anthropogenic causes, *Clim. Dyn.*, *17*, 1–21, 2001.

Stott, P. A., M. R. Allen, and G. S. Jones, Estimating signal amplitudes in optimal fingerprinting, part ii, Application to general ciculation models, *Clim. Dyn.*, in press, 2003a.

Stott, P., G. Jones, and J. Mitchell, Do models underestimate the solar contribution to recent climate change?, *J. Clim.*, in press, 2003b.

Tett, S. F. B., J. F. B. Mitchell, D. E. Parker, and M. R. Allen, Human influence on the atmospheric vertical temperature structure: Detection and observations, *Science*, *247*, 1170–1173, 1996.

Tett, S. F. B., P. A. Stott, M. R. Allen, W. J. Ingram, and J. F. B. Mitchell, Causes of twentieth century temperature change, *Nature*, *399*, 569–572, 1999.

Tett, S. F. B., et al., Estimation of natural and anthropogenic contributions to 20th century temperature change, *J. Geophys. Res.*, *107*(D16), 4306, doi:10.1029/2000JD000028, 2002.

G. S. Jones, S. F. B. Tett, and P. A. Stott, Met Office, Hadley Centre for Climate Prediction and Research, London road, Bracknell RG12 2SZ, UK. (gareth.s.jones@metoffice.com)